GEOPHYSICAL RESEARCH LETTERS, VOL. 37, L13603, doi:10.1029/2010GL043159, 2010

Sea breeze forcing of estuary turbulence and air-water CO_2 exchange

Philip M. Orton,[1,2] Wade R. McGillis,[1,3] and Christopher J. Zappa[1]

Received 5 March 2010; revised 9 May 2010; accepted 1 June 2010; published 9 July 2010.

[1] The sea breeze is often a dominant meteorological feature at the coastline, but little is known about its estuarine impacts. Measurements at an anchored catamaran and meteorological stations along the Hudson River and New York Bay estuarine system are used to illustrate some basic characteristics and impacts of the feature. The sea breeze propagates inland, arriving in phase with peak solar forcing at seaward stations, but several hours later at up-estuary stations. Passage of the sea breeze front raises the water-to-air CO_2 flux by 1–2 orders of magnitude, and drives turbulence comparable to spring tide levels in the upper meter of the water column, where most primary productivity occurs in this highly turbid system. Modeling and observational studies often use remotely-measured winds to compute air-water fluxes (e.g., momentum, CO_2), and this leads to a factor of two flux error on sea breeze days during the study. **Citation:** Orton, P. M., W. R. McGillis, and C. J. Zappa (2010), Sea breeze forcing of estuary turbulence and air-water CO_2 exchange, *Geophys. Res. Lett.*, *37*, L13603, doi:10.1029/2010GL043159.

1. Introduction

[2] The sea breeze is a ubiquitous fair-weather feature along most of the world's coastlines, present in warmer months at mid-latitudes, and year-round in tropical and subtropical regions [*Gille et al.*, 2003]. It arises on sunny days due to atmospheric pressure differences that develop as a result of the different solar absorption properties of sea and land. If no topographic boundaries exist, the sea breeze often penetrates tens of kilometers inland, and at some locations, hundreds of kilometers [*Miller et al.*, 2003].

[3] Estuarine air-water gas exchange and biogeochemistry are gaining increased attention due to their potential role in the global carbon cycle [e.g., *Dai et al.*, 2009], as well as concerns over poorly-ventilated, low-oxygen bottom water. Air-water exchanges are often primarily controlled by winds [*Wanninkhof*, 1992], so the sea breeze likely plays an important role with these processes. Moreover, recent studies have begun to demonstrate powerful influences of the sea breeze on circulation, freshwater residence time, and in some cases mixed layer depth in estuaries [*Geyer*, 1997; *Simionato et al.*, 2005], coastal embayments [*Valle-Levinson et al.*, 2003], and river plumes [*Hunter et al.*, 2007].

[4] Here, we present first-of-their-kind observations of the inland propagation of the sea breeze past four sites along an estuary, and detailed measurements of associated air-water CO_2 exchange and water turbulence. We demonstrate the air-water flux errors that can arise from using remote wind data or daily averages in modeling or observational studies of systems with sea breezes. We conclude by using spectral analysis to look at seasonality and quantify the proportion of wind variance in the diurnal band, and briefly discuss systems likely to have similar sea breeze impacts.

2. Field Observations

[5] A 1.85 m long Self-Orienting Catamaran (SOCa) with air-water exchange and turbulence measurements was anchored frequently at a 5.1 m deep site on the Hudson River estuary from 23 September through 2 November, 2007 (year-day 265.0–306.0 (Figure 1)). An acoustic Doppler velocimeter mounted on a forward boom sampled water velocity at 50 cm depth at 25 Hz, and the Inertial Dissipation Method (IDM) was used with the frozen field assumption to estimate 10 minute averages of the rate of dissipation (ε) of turbulent energy [*Orton*, 2010; *Zappa et al.*, 2003]. A keel rotated SOCa so that the boom was oriented into the current to avoid wake biases. Periods with a wave orbital speed greater than 40% of mean flow speed were omitted to avoid biases from aliasing of wave energy into the inertial subrange [*Lumley and Terray*, 1983]. Nearby, a bottom-mounted acoustic Doppler current profiler (ADCP) measured vertical profiles of velocity at 1 Hz and 25 cm vertical resolution, permitting computation of shear production (P) of turbulent energy [e.g., *Orton and Visbeck*, 2009]. Five 12-hour time series with vertical CTD profiling (salinity, temperature) were also performed from a small anchored boat.

[6] SOCa also provided automated CO_2 profiling using a gas valve switching system, and water-to-air CO_2 flux (F_{CO2}) estimates using the Gradient Flux Technique (GFT) [*Orton*, 2010; *Zappa et al.*, 2003]. The profiling system measured CO_2 partial pressure (pCO_2) using a non-dispersive infrared sensor (NDIR), sampling air from atmospheric heights of 0.4 and 2.25 m and from the headspace of an equilibrator receiving pumped surface water (0.2 m depth). Timeseries measurements were made of wind and air temperature with a sonic anemometer (height 1.2 m), humidity and pCO_2 with an NDIR (height 2.25 m), and water temperature (depth 0.2 m). GFT utilizes the fact that a constituent's air-water exchange is proportional to its vertical gradient in the atmospheric surface layer, and corrects for the smearing of the gradient by turbulent mixing. The

[1] Lamont-Doherty Earth Observatory, Earth Institute at Columbia University, Palisades, New York, USA.
[2] Earth and Environmental Sciences, Columbia University, New York, New York, USA.
[3] Earth and Environmental Engineering, Columbia University, New York, New York, USA.

0094-8276/10/2010GL043159

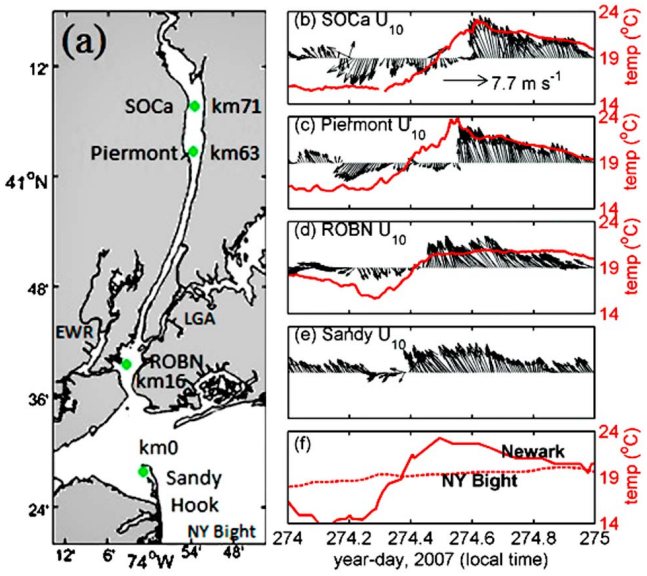

Figure 1. Study area map, with wind and air temperature data for a strong sea breeze day. (a) The Hudson River and New York Bay estuarine system, showing the Sandy Hook, Robbins' Reef (ROBN), and Piermont Pier meteorological stations, and the SOCa catamaran location. Wind velocity vectors and local air temperature data are shown on the right: at (b) SOCa, (c) Piermont, (d) ROBN, and (e) Sandy Hook, rotated by 30° clockwise to account for the different principal axis of the diurnal winds at that site. (f) Air temperatures over the coastal Atlantic Ocean in New York Bight (NOAA buoy 44025, 40°15′N, 73°10′W) and inland at Newark (EWR). Similar wind patterns were typically also observed at LaGuardia Airport (LGA).

required air-water heat and momentum fluxes and Monin-Obukhov Similarity Theory parameterizations of turbulent diffusivity were all computed using the MATLAB COARE 3.0 bulk flux toolbox [*Fairall et al.*, 2003].

[7] Additional measurements utilized in this paper include our own meteorological station at Piermont Pier (anemometer at 8 m height), and National Data Buoy Center (NDBC) stations at Robbins Reef lighthouse in Upper New York Bay (code ROBN, anemometer at 22 m height) and Sandy Hook (code SDHN, at 9 m height), all mapped in Figure 1. Our Piermont Pier station is a tripod on top of a one-story flat-top building, with measurements that include a cup/vane anemometer at 8 m height above mean water level, solar radiation and air temperature. When inter-compared in this paper, wind data are transformed to 10 m height wind (U_{10}) by assuming neutral atmospheric conditions and a sea surface aerodynamic roughness length of 3×10^{-4} m, an approximation for ~6 m s^{-1} along-channel winds and ~30 cm wind seas [*Drennan et al.*, 2005], typical of the Hudson's sea breeze. Uncertainty of a factor of 10 in roughness leads to uncertainty in the U_{10} estimates of only ±10% or less, and almost no error for the sites near 10 m height.

[8] Sea breeze days are defined using a three-stage conditional filter similar to that of *Furberg et al.* [2002], designed to identify days with a daytime onset of a surface onshore wind that is related to the cross-shore air temperature gradient. The stages require that (1) the sunrise-to-sunset mean air temperature over land must be greater than the temperature over the sea, (2) the wind must blow onshore for at least two hours between [sunrise +2h] to [sunset +2h], and (3) a majority of winds from [sunrise −8h] to [sunrise +2h] must be calm (below 2 m s^{-1}) or offshore.

3. Results and Discussion

[9] On sunny, warm days during the field study, a land-sea temperature gradient built up by mid-morning and wind observations showed characteristics of a sea breeze, with south winds arriving at the measurement sites by mid-afternoon (Figure 1). Cooling or moderating temperatures often followed the arrival of the south winds. There were a total of seven sea breeze days, year-days 269, 272, 274, 275, 276, 277 and 279, for which the general pattern and estuarine impacts of winds are described below.

[10] There was often a well-defined up-estuary delay in arrival of the south wind, to at least the furthest station northward, 71 km up-estuary (Figures 1–2). This suggests the marine layer was propagating as a gravity current, as sea breezes typically do over land [*Miller et al.*, 2003] and land breezes over the ocean [*Gille et al.*, 2005]. Moreover, wind and temperature changes were often abrupt, suggesting a front formed at the leading edge, an additional feature of sea breezes and gravity currents [*Miller et al.*, 2003]. The sea breeze wind pattern was typically also present at LaGuardia Airport (LGA; Figure 1), so the marine layer may have traveled the over-land route northward past LaGuardia to get to Piermont, or up the steep-walled Hudson which is bordered by 100 m or greater topography and infrastructure in most places.

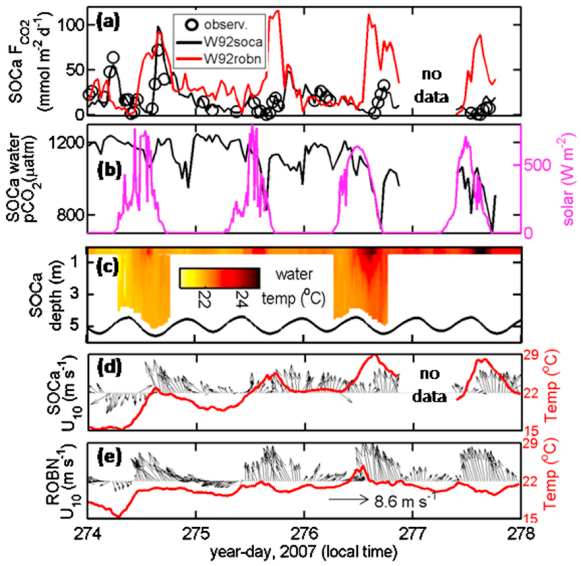

Figure 2. Observations during the same period shown in Figure 1 and the subsequent three days: (a) water-to-air CO_2 flux estimates (F_{CO2}) including SOCa observations, as well as those computed from a quadratic wind-based parameterization [*Wanninkhof*, 1992] with local winds (W92soca) or remote winds (W92robn), (b) SOCa water-side CO_2 partial pressure (pCO_2) and solar radiation, (c) water temperature (shading) and depth (black line), and (d, e) wind velocity vectors and air temperatures at SOCa and ROBN.

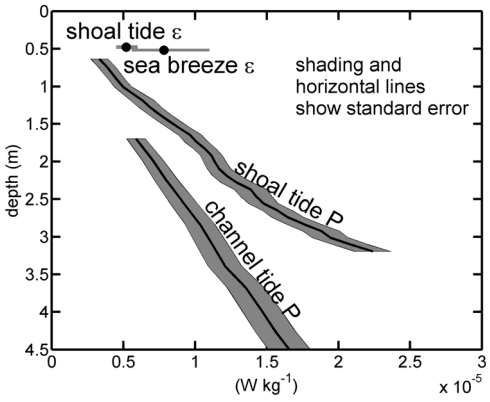

Figure 3. Comparison of turbulence levels resulting from sea breezes and spring tides. Average near-surface dissipation (ε) and shear production (P) are shown for peak spring tide currents over the shoal at SOCa ("shoal tide") and peak spring tide currents over the deep channel ("channel tide"), and compared with periods with typical peak sea breeze wind speeds of 5.0–7.7 m s^{-1}. Sea breeze P is not shown because waves bias the P measurement, and channel tide ε was not measured.

[11] The observed lag of the sea breeze with distance up the Hudson is useful for estimating marine layer height by inverting the gravity wave propagation speed equation, $U_{sb} = \gamma(g'h)^{0.5}$, where h is a scale height, $g' = g(\Delta\theta/\theta)$ is the reduced gravity, $\Delta\theta$ is the inversion strength, θ is atmospheric potential temperature in Kelvin, and γ is ~0.62 [*Gille et al.*, 2005]. The lags in arrival of the wind front over the 55 km distance from ROBN to SOCa, were 3.34 and 3.64 h on year-days 274 and 277, suggesting propagation speeds of 4.6 and 4.2 m s^{-1}, respectively. Using these speeds with the observed afternoon mean land-sea temperature difference of 3°C (Figure 1f) and 6°C gives scale heights (h) of 470 and 280 m. Prior observations of New York area sea breeze inversion heights have been from 100–300 m [*Childs and Raman*, 2005; *Novak and Colle*, 2006; *Thompson et al.*, 2007]. The higher h on year-day 274 may explain the relatively robust inland propagation on that day, making the feature less sensitive to urban roughness elements that have been shown to slow propagation [*Childs and Raman*, 2005].

3.1. Sea Breeze Driven Turbulence and Air-Water CO_2 Exchange

[12] The diurnal wind cycle had a dominant effect on the water-to-air CO_2 flux (F_{CO2}) on sea breeze days during the study (Figure 2). From Piermont northward, sea breeze days typically had light winds in the middle of the day, with glassy or light chop sea surface conditions and SOCa F_{CO2} values below 5 mmol m^{-2} d^{-1}. When the sea breeze arrived at SOCa (U_{10} = 5.0–7.7 m s^{-1}), wind wave breaking was often observed, and F_{CO2} rose by a factor of 10–100 to as much as 73 mmol m^{-2} d^{-1}.

[13] The sea breeze can drive near-surface turbulence comparable to spring tide levels, but with daily recurrence (Figure 3). Mean dissipation rates (ε) at 50 cm depth associated with 5.0–7.7 m s^{-1} winds (U_{10}) and weak currents (below 0.4 m s^{-1}) during the entire study were 8.0×10^{-6} W kg^{-1}. These are comparable to ε at the same depth during peak spring tides with weak winds (U_{10} below 4 m s^{-1}), which averaged 5.2×10^{-6} W kg^{-1}. Peak spring tide is defined as periods within two days of the month's strongest spring tide, with depth-average ebb tide currents from 80–100% of tidal maxima (spring ebbs had stronger near-surface turbulence than floods). The turbulent shear production rate (P) is closely related to and typically scales with ε [e.g., *Gross and Nowell*, 1985], and the average spring tide upper water column P is also similar to the sea breeze driven ε. The shoal site where SOCa was deployed is 5.1 m deep, but a 100-day current profiler deployment east of Piermont Pier in the Hudson's deep channel (14 m) where currents are stronger [*Orton and Visbeck*, 2009] exhibits similar upper water column P levels (Figure 3). For comparison, wall-layer modeled dissipation levels at 50 cm depth for a quadratic drag coefficient of 0.0012 and winds from 5.0–7.7 m s^{-1} are 1.1–4.1×10^{-6} W kg^{-1}, but additional superimposed processes (e.g., wind wave breaking) likely explain the higher observed sea breeze driven ε.

[14] The diurnal phasing of the sea breeze is particularly interesting in light of diurnal cycles of solar heating, solar heating enhanced stratification, and primary production. The Hudson is turbid, 90% of light is often attenuated in the upper meter, and light limitation has been shown to be a very important control on photosynthesis [*Malone*, 1977]. Calm waters at mid-day enabled solar heating to warm surface waters by up to 2.2°C (Figure 2), and the vertical temperature gradient typically enhanced density stratification by 50–100%, relative to salinity stratification alone. Water pCO_2 at 20 cm depth decreased during these periods by as much as 42% (year-day 276.5–276.7 (Figure 2)). This was likely due to primary production, as a 2°C change in temperature would only result in a 5% change in CO_2 solubility [*Wanninkhof*, 1992].

3.2. Errors From Under-Sampling or Using Remote Winds

[15] Modeling and observational studies often use remote [e.g., *Hellweger et al.*, 2004; *Yan et al.*, 2008] or daily-average [e.g., *Yan et al.*, 2008] wind forcing to parameterize air-water exchanges, or measure gas exchange on daily or often longer timescales with deliberate chemical tracer injection. Using remote wind data with a quadratic parameterization can lead to large errors in estimated air-water exchanges (e.g., CO_2, momentum). The Figure 2a shows four days of measured F_{CO2} at the SOCa site, compared with estimates from a quadratic wind-based parameterization using local winds [*Wanninkhof*, 1992], and from the parameterization using remote wind data measured at the ROBN station. Using the parameterization with local winds for all the sea breeze days gives a net F_{CO2} estimate 5% above the *in situ* measurements, whereas using the parameterization with remote winds gives a net F_{CO2} estimate 92% above the *in situ* measurements and marked differences in diurnal phasing of the flux. Until 2006, there were no operational wind data measurements on the Hudson or New York Bay, and this is still common for many estuaries.

[16] Using daily averages will obscure diurnal phasing effects important to biogeochemical processes, and can lead to overestimation of the net flux. The timing of the sea breeze can reduce the net F_{CO2}, relative to steady winds, if it arrives at the time of day that photosynthesis has minimized the surface water pCO_2 (e.g., year-day 276.7). Moreover,

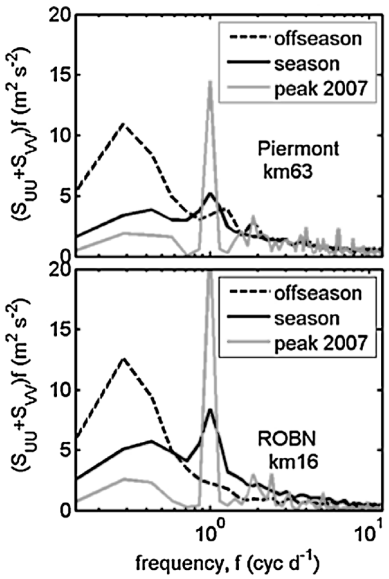

Figure 4. Variance-preserving wind velocity spectra for two sites along the Hudson/NY Bay estuarine system. Analysis periods include sea breeze "season" from April–August, 2009; "offseason" from January–February, 2009; and "peak 2007" from year-day 272.0–279.0 during the field study.

new measurements from August 2009 at Piermont Pier show that pCO_2 there can vary from highly supersaturated (2000 μatm) to highly undersaturated (200 μatm) from early morning to late afternoon, along with supersaturation of oxygen. Strong diurnal cycles in pCO_2 have also been observed in other estuaries [e.g., *Dai et al.*, 2009].

3.3. Broader Context

[17] The seasonality and along-estuary variation of diurnal band winds are illustrated with wind velocity spectra in Figure 4. Diurnal band winds can dominate the wind variability on the Hudson for as much as a week at a time in spring, summer or early fall. Integrating the spectra, the diurnal band ($0.75 < f < 1.3$ cyc d^{-1}) provides 20% of total wind variance at both ROBN and Piermont during sea breeze season. Viewing all the available data from these sites, the sea breeze is a more reliable mid-day and afternoon feature at Robbins Reef and Sandy Hook. At Piermont, the phase lag and duration of the sea breeze are highly erratic, and the reverse process, the land breeze, provides some of the diurnal wind energy. The erratic phase lag is likely due to the long propagation distance to that site, as many prior studies have shown a high level of sensitivity of deep inland propagation to ambient synoptic winds [*Miller et al.*, 2003].

[18] Sea breezes are a common and in some cases powerful forcing agent in many estuaries and coastal regions [e.g., *Geyer*, 1997; *Hunter et al.*, 2007; *Simionato et al.*, 2005; *Valle-Levinson et al.*, 2003], many of which likely exhibit similar impacts on air-water exchanges and turbulence to those reported here. A quick survey of a few other estuaries with good NDBC buoy coverage shows that the Strait of Juan de Fuca is a system with stronger sea breezes (often 10 m s^{-1}) and more robust and predictable inland propagation, likely due to strong topographic trapping of the marine layer by mountains to the north and south. A common summertime wind pattern is that west winds are maximal at ~1700 h local time near the ocean and maximal at ~2200 h at the eastern end of the Strait, consistent with propagation at 8.0 m s^{-1}.

[19] In conclusion, we have demonstrated that the sea breeze propagates inland and can reach at least 71 km up the Hudson/NY Bay estuarine system. Sea breeze winds can raise F_{CO2} by 1–2 orders of magnitude, and raise turbulence levels in the upper meter of the water column to spring tide levels on a daily recurring basis. Using remote wind data from the nearest NDBC site in a quadratic wind-based parameterization led to overestimation of F_{CO2} by 92% for sea breeze days during the study, due to strong spatial wind variability. These results demonstrate that physical and biogeochemical studies for certain estuaries should measure or model atmospheric forcing on spatial and temporal scales necessary to resolve propagating sea breezes.

[20] **Acknowledgments.** The authors would like to thank Bob Houghton, Tobias Kukulka and an anonymous reviewer for insightful critiques. This research was funded by National Science Foundation grant 0526677. Lamont-Doherty Earth Observatory contribution 7372.

References

Childs, P. P., and S. Raman (2005), Observations and numerical simulations of urban heat island and sea breeze circulations over New York City, *Pure Appl. Geophys.*, *162*(10), 1955–1980, doi:10.1007/s00024-005-2700-0.

Dai, M., Z. Lu, W. Zhai, B. Chen, Z. Cao, K. Zhou, W.-J. Cai, and C.-T. A. Chen (2009), Diurnal variations of surface seawater pCO_2 in contrasting coastal environments, *Limnol. Oceanogr.*, *54*(3), 735–745.

Drennan, W. M., P. K. Taylor, and M. J. Yelland (2005), Parameterizing the sea surface roughness, *J. Phys. Oceanogr.*, *35*(5), 835–848, doi:10.1175/JPO2704.1.

Fairall, C. W., E. F. Bradley, J. E. Hare, A. A. Grachev, and J. B. Edson (2003), Bulk parameterization of air-sea fluxes: Updates and verification for the COARE algorithm, *J. Clim.*, *16*(4), 571–591, doi:10.1175/1520-0442(2003)016<0571:BPOASF>2.0.CO;2.

Furberg, M., D. G. Steyn, and M. Baldi (2002), The climatology of sea breezes on Sardinia, *Int. J. Climatol.*, *22*(8), 917–932, doi:10.1002/joc.780.

Geyer, W. R. (1997), Influence of wind on dynamics and flushing of shallow estuaries, *Estuarine Coastal Shelf Sci.*, *44*(6), 713–722, doi:10.1006/ecss.1996.0140.

Gille, S. T., S. G. Llewellyn Smith, and S. M. Lee (2003), Measuring the sea breeze from QuikSCAT scatterometry, *Geophys. Res. Lett.*, *30*(3), 1114, doi:10.1029/2002GL016230.

Gille, S. T., S. G. Llewellyn Smith, and N. M. Statom (2005), Global observations of the land breeze, *Geophys. Res. Lett.*, *32*, L05605, doi:10.1029/2004GL022139.

Gross, T., and A. Nowell (1985), Spectral scaling in a tidal boundary layer, *J. Phys. Oceanogr.*, *15*(5), 496–508, doi:10.1175/1520-0485(1985)015<0496:SSIATB>2.0.CO;2.

Hellweger, F., A. Blumberg, P. Schlosser, D. Ho, T. Caplow, U. Lall, and H. Li (2004), Transport in the Hudson estuary: A modeling study of estuarine circulation and tidal trapping, *Estuaries Coasts*, *27*(3), 527–538, doi:10.1007/BF02803544.

Hunter, E., R. Chant, L. Bowers, S. Glenn, and J. Kohut (2007), Spatial and temporal variability of diurnal wind forcing in the coastal ocean, *Geophys. Res. Lett.*, *34*, L03607, doi:10.1029/2006GL028945.

Lumley, J. L., and E. A. Terray (1983), Kinematics of turbulence converted by a random wave field, *J. Phys. Oceanogr.*, *13*, 2000–2007, doi:10.1175/1520-0485(1983)013<2000:KOTCBA>2.0.CO;2.

Malone, T. C. (1977), Environmental regulation of phytoplankton productivity in the lower Hudson estuary, *Estuarine Coastal Mar. Sci.*, *5*(2), 157–171, doi:10.1016/0302-3524(77)90014-7.

Miller, S. T. K., B. D. Keim, R. W. Talbot, and H. Mao (2003), Sea breeze: Structure, forecasting, and impacts, *Rev. Geophys.*, *41*(3), 1011, doi:10.1029/2003RG000124.

Novak, D. R., and B. A. Colle (2006), Observations of multiple sea breeze boundaries during an unseasonably warm day in metropolitan New York City, *Bull. Am. Meteorol. Soc.*, *87*(2), 169–174, doi:10.1175/BAMS-87-2-169.

Orton, P. M. (2010), Estuary turbulence and air-water CO_2 exchange, Ph.D. dissertation thesis, 211 pp., Columbia Univ., New York.

Orton, P. M., and M. Visbeck (2009), Variability of internally generated turbulence in an estuary, from 100 days of continuous observations, *Cont. Shelf Res.*, *29*(1), 61–77, doi:10.1016/j.csr.2007.07.008.

Simionato, C. G., V. Meccia, W. Dragani, and M. Nuñez (2005), Barotropic tide and baroclinic waves observations in the Río de la Plata Estuary, *J. Geophys. Res.*, *110*, C06008, doi:10.1029/2004JC002842.

Thompson, W. T., T. Holt, and J. Pullen (2007), Investigation of a sea breeze front in an urban environment, *Q. J. R. Meteorol. Soc.*, *133*(624), 579–594, doi:10.1002/qj.52.

Valle-Levinson, A., L. P. Atkinson, D. Figueroa, and L. Castro (2003), Flow induced by upwelling winds in an equatorward facing bay: Gulf of Arauco, Chile, *J. Geophys. Res.*, *108*(C2), 3054, doi:10.1029/2001JC001272.

Wanninkhof, R. (1992), Relationship between wind speed and gas exchange over the ocean, *J. Geophys. Res.*, *97*(C5), 7373–7382, doi:10.1029/92JC00188.

Yan, S., L. A. Rodenburg, J. Dachs, and S. J. Eisenreich (2008), Seasonal air-water exchange fluxes of polychlorinated biphenyls in the Hudson River estuary, *Environ. Pollut.*, *152*(2), 443–451, doi:10.1016/j.envpol.2007.06.074.

Zappa, C. J., P. A. Raymond, E. Terray, and W. R. McGillis (2003), Variation in surface turbulence and the gas transfer velocity over a tidal cycle in a macro-tidal estuary, *Estuaries*, *26*(6), 1401–1415, doi:10.1007/BF02803649.

W. R. McGillis, P. M. Orton, and C. J. Zappa, Lamont-Doherty Earth Observatory, Earth Institute at Columbia University, 61 Rte. 9W, Palisades, NY 10964, USA. (orton@ldeo.columbia.edu)